

Where's the Disk?: LBV bubbles and Aspherical Fast Winds

Adam Frank

*Department of Physics and Astronomy, University of Rochester,
Rochester, NY 14627-0171;
email: afrank@alethea.pas.rochester.edu*

Abstract. Previous studies have explained the shapes of LBV nebulae, such as η Car, by invoking the interaction of an isotropic fast wind with a previously deposited, slow *aspherical* wind (a "slow torus"). In this work I focus on the opposite scenario where an aspherical fast wind expands into a previously deposited *isotropic* slow wind. Using high resolution hydrodynamic simulations which include the effects of radiative cooling I have completed a series of numerical experiments to test if and how aspherical fast winds effects wind blown bubble morphologies. The simulations demonstrate that aspherical fast winds can produce strongly bipolar outflows and recover some important aspects of LBV bubbles which the previous models can not.

1. Introduction

In just a few years the HST has transformed our understanding of the massive unstable stars know as Luminous Blue Variables (LBVs). Recent observations have revealed a number of LBVs or LBV candidates to be surrounded by extended *aspherical* outflows. The most extraordinary of these is the markedly bipolar nebula surrounding η Carinae ("the homunculus": Hester *et al.* 1991, Ebbets *et al.* 1993, Humphreys & Davidson 1994). Other LBVs show nebulae with varying degrees of asphericity from elliptical (R127, Nota *et al.* 1995) to strongly bipolar (which we define though the presence of an equatorial waist: HR Carinae; Nota *et al.* 1995; Weis *et al.* 1996).

These bipolar morphologies are quite similar to what has been observed in Planetary Nebulae (PNe) which arise from low mass stars (Manchado *et al.* 1996). The aspherical shapes of PNe have been successfully explained through a scenario termed the "Generalized Interacting Stellar Winds" model (GISW, Frank & Mellema 1994) where an isotropic fast wind from the central star (a proto-white dwarf) expands into an aspherical (toroidal) slow wind ejected by the star in its previous incarnation as a Asymptotic Red Giant. High densities in the equatorial plane of the AGB outflow constrain the expansion of the fast wind. The expanding shock wave which results from the wind/wind interaction quickly assumes a elliptical prolate geometry. If the ratio of mass density between the equator and pole (a parameter we call q , $q_p = \rho_e/\rho_p$) is high enough, then the elliptical bubble eventually develops a waist and becomes bipolar.

The similarity of PNe and LBV nebulae has led to the suggestion that both families of objects are shaped in similar ways. In Frank, Balick, & Davidson 1995 (hereafter: FBD) a GISW model for η Car was presented in which a spherical “outburst” wind expelled during the ≈ 1840 outburst expanded into a toroidal “pre-outburst” wind. FBD showed that the resulting bipolar outflow could recover both the gross morphology and kinematics of the Homunculus. Nota *et al.* 1995 (hereafter NLCS) used a similar model for other LBV nebulae presenting a unified picture of the development of LBV outflows. More recently Mac Low, Langer & Garcia-Segura 1996 (hereafter MLG) presented a model which also relied on the GISW scenario but which changed the order of importance of the winds. Using the Wind Compressed Disk model of Bjorkman & Cassinelli 1992 MLG showed that a strong equator to pole density contrast would likely form *during the outburst*. In MLG’s model it is the post-outburst wind which “inflates” the bipolar bubble via its interaction with the toroidal outburst wind.

While all these models have demonstrated the potential efficacy of the GISW scenario via a reliance on a slow torus they are troubling in their mutual inconsistency. Specifically the question - “Where is the disk (torus)?” - must be answered. Does the torus form during the LBV eruption as in MLG or does it form during the pre-eruption wind as in FBD and NLCS?

Stepping back further one can also ask if a disk is needed at all? The latter question arises from consideration of new HST images of η Car (Morse *et al.* 96) which reveal the equatorial “disk” to be so highly fragmented that it may be more reasonable to consider it a “skirt” of individual clumps of ejecta rather than an azimuthally continuous structure. This point is crucial since an equatorial spray of isolated bullets can not hydrodynamically constrain an isotropic stellar wind to form a bipolar outflow. Thus we are led to consider an alternative model to that proposed by FBD, NLCS and MGL. Here we further generalize the GISW model by turning that scenario on its head. In what follows we consider the case of an *aspherical fast wind* interacting with a *isotropic slow wind*. We imagine a fast wind ejected with higher velocity along the poles than along the equator. The question we wish to answer is: can such a wind, expanding into an isotropic environment, account for the shapes of LBV nebulae.

Theoretical models admit the possibility of aspherical fast winds in massive stars (Lamers & Pauldrach 1991). More importantly, there is direct evidence for asphericity in LBV winds. Observations of the wind of AG Carinae (Leitherer *et al.* 1994) imply a pattern of densities and velocities from pole to equator much like that described in Lamers & Pauldrach 1991. Finally we note that it is worthwhile to pursue this kind of investigation simply because it has not been done before. The GISW model and its variations has been very successful in accounting for a variety of bipolar outflow phenomena (Blondin & Lundqvist 1993; Frank, Balick & Livio 1996; Frank & Mellema 1996,). Since the effect of aspherical fast winds has yet to be investigated the potential of finding useful results is high which is argument enough for a detailed study.

2. Computational Methods and Initial Conditions

The details of the computational method and initial conditions can be found elsewhere (Frank, Ryu & Davidson 1997). Here we present only a brief overview.

We model the gasdynamic interactions via the Euler equations with a radiation loss ‘sink’ term in the energy equation.

Our numerical experiments are designed to study the evolution of wind-blown bubbles driven by aspherical fast winds. The environment is always assumed to be characteristic of a previously deposited spherically symmetric “pre-outburst” wind which we denote as wind 0 with mass loss rate \dot{M}_0 and velocity V_0 . For the driving “fast” or “outburst” wind, which we denote as wind 1, we need a formalism for setting the latitudinal (θ) variations in the wind properties i.e. $\dot{M}_1 = \dot{M}_1(\theta)$ and $V_1 = V_1(\theta)$. We note that since we wish to drive prolate bipolar bubbles we always assume that the velocity at the poles is larger than at the equator. We have also explore models with a “post-outburst” wind (denoted as wind 2)

We have chosen to explore different scenarios for the pole to equator variation in wind parameters. Each scenario is based on assuming a different quantity remain constant across the face of the star. They are: Constant Momentum Input ($\dot{\Pi} = \dot{M}_1 V_1 = \text{Const}$); Constant Energy Input ($\dot{E} = \frac{1}{2} \dot{M}_1 V_1^2 = \text{Const}$); Constant density ($\rho_1 = \text{Const}$).

If we choose our fiducial values for the density and velocity at the equator (ρ_{1e}, V_{1e}), the latitudinal variation can be expressed as powers of an ad hoc function $f(\theta)$ which produces a smooth variation in V_1 and ρ_1 from equator to pole. Using the formalism described above we have carried out three sets of numerical experiments varying the ratio of mass loss rates in the successive winds between each set. Within the first two sets we performed three simulations with $\dot{M}_1(\theta)$ and $V_1(\theta)$ corresponding to the scenarios discussed above. In the final set only the $\dot{\Pi} = \text{Const}$ case was used and the equator to pole velocity contrast $q_v = V_{1e}/V_{1p}$ was varied. The initial conditions for each of our 9 simulations are shown in table 1.

Table 1. Initial Conditions For Runs A - H

run	\dot{M}_0	V_0	\dot{M}_{1e}	V_{1e}	\dot{M}_2	V_2	q_v
A-C	1×10^{-4}	100	1×10^{-4}	150	NA	NA	0.2
D-F	1×10^{-6}	100	1×10^{-4}	150	NA	NA	0.2
G	1×10^{-6}	100	1×10^{-4}	150	1×10^{-6}	1400	0.3
H	1×10^{-6}	100	1×10^{-4}	150	1×10^{-6}	1400	0.14
I	1×10^{-6}	100	1×10^{-4}	150	1×10^{-6}	1400	0.1

3. Results

3.1. 2 Wind Models with $\dot{M}_0 = \dot{M}_{1e}$

In Experiment 1 we examined the interaction between two winds of with the same mass loss rate. These simulations are performed to give us a baseline on the gas-dynamic flow pattern. The results of these simulations are shown in the top row of Fig 1 where we present grayscale maps of $\text{Log}_{10}(\rho)$ for models A ($\dot{\Pi} = \text{Const}$), B ($\dot{E} = \text{Const}$), and C ($\rho = \text{Const}$). Fig 1 shows that in all

three scenarios the shell of swept-up pre-outburst material becomes significantly aspherical due to the aspherical driving force of the outburst wind. Notice also that the bubbles all develop a “waist” - the observational signature of a bipolar, rather than elliptical, configuration. Model C has the highest global outburst wind density demonstrating that the degree of bipolarity depends on relative densities between the aspherical outburst and spherically symmetric pre-outburst winds.

3.2. 2 Wind Models with $\dot{M}_{1e} > \dot{M}_0$

As Langer *et al.* 1994 have demonstrated the LBV outburst phase is likely to involve an increase in mass loss over the pre-outburst wind. Thus we have the case of a “heavy” wind expanding into a light one. To explore this situation we have run a second set of experiments, runs D, E, & F, where $\dot{M}_{1e} = 100\dot{M}_0$. The results of these simulations are shown in the second row of Fig 1.

The bubbles formed in these runs are more strongly bipolar than those in the previous experiment. The reason for this is the relatively small effect of the ambient medium in decelerating the massive winds (deceleration does however occur). Runs E and F show similar morphologies as was the case in the first set of experiments. Similarly the $\rho = Const$ case again produces the most bipolar configuration because of the density is high across the face of the star. Fig 1 demonstrates the principle conclusion of our first two sets of experiments. *An aspherical stellar wind can drive an aspherical bubble.*

3.3. 3 Wind Models

In runs G, H, and I we have performed simulations similar to run D. In the new simulations the outburst wind lasted only 30 years. Afterwards a post-outburst wind was driven into the grid. The characteristics of the post-outburst wind were meant to qualitatively mimic the conditions currently observed in η Carinae. We used a relatively low mass rate, high velocity post-outburst wind i.e. $\dot{M}_2 < \dot{M}_{1e}$ and $V_2 > V_{1e}$. Thus in these simulations (each of which has a different equator to pole velocity contrast) we are interested the effect of the post-outburst wind on a bipolar bubble created by the previously ejected dense aspherical outburst wind.

In the last row of Fig 1 we present $\log_{10}(\rho)$ maps for all three simulations in these experiments. Runs G,H, and I with $q_v = 1/3, 1/7$ and $1/10$ all produce strong bipolar morphologies which develop without the need for a slow-moving disk. Comparison between the simulations shows that decreasing q_v produces stronger bipolar morphologies. It is worth noting that if the expansion of the bubble were ballistic we would expect the shape of the bubbles to scale with q_v . Since this is not the case the bubbles must experience significant hydrodynamic shaping (i.e. what you put in is not what you get out). Some part of the shaping is due to deceleration of the outburst wind via the previously ejected material. The post-outburst wind however also contributes by accelerating the the outburst material. As the bubble evolves this acceleration will have its greatest effect near the equator where the outburst wind has been most strongly decelerated. Thus the action of the post-outburst wind will be to drive the bubble towards a more spherical configuration as system evolves.

4. Discussion and Conclusions

Our simulations demonstrate that bipolar wind blown bubbles can result purely from the action of an aspherical fast wind. In previous studies of LBV bubbles (FBD, NLCS, MLG) it has been assumed that a slow moving torus or disk of gas must exist first for a successive spherical fast wind to shape into a bipolar configuration. Our results indicate that the properties of LBV bubbles may not require such a torus to form either before (FBD, NLCS) or during (MLG) the outburst.

Thus we are faced with an abundance of models to explain the same phenomena. Resolving the issue of if a disk is needed may require observations of the angular profiles of mass and momentum in LBV shells (such an approach has been successfully used for YSOs bipolar bubbles; Masson & Chernin 1992)

Acknowledgments Support for this work was provided by NASA grant HS-01070.01-94A from the Space Telescope Science Institute, which is operated by AURA Inc under NASA contract NASA-26555. Additional support came from the Minnesota Supercomputer Institute.

Discussion

Dr. Ignace: Aside from η Car are you suggesting that the brightness enhancements around, say, AG Car and R127, are from dense polar caps instead of a dense waist and as a discriminant would you predict the caps to be expanding faster than the equator.

Frank: The waist may still appear brighter because emission is a density squared process but you are right that the kinematical pattern for these kinds of bubbles may be different from the slow torus version of the bipolar bubble.

Dr. Owocki: It is interesting that you get the best agreement with the shape of η Car when you use an constant density wind. Radiation driven winds from rotating stars with gravity darkening predict higher densities at the pole so I suggest you explore that case two.

Frank: In such a case an even more bipolar bubble would be expected since you are increasing the ram pressure at the pole. I will include that in my future models.

Dr. Langer: I wonder if a fast dense outburst wind is compatible with the models: firstly if the outbursts are related to surface instabilities the escape velocity goes to zero and the winds would be slow. There would also be an energy problem: the kinetic flux might overwhelm the stellar luminosity.

Frank: Well fast and slow are relative concepts. All I am asking is that an aspherical outburst wind drive the shape of the nebula. I use velocities as low as 100 km/s in my models. I don't intrinsically need V_{wind} to be an order of magnitude higher. Also the pre-outburst wind may be relatively fast and have left a shocked bubble behind which will still provide an isotropic back-pressure.

Dr. Schulte-Ladbeck: What was the geometry of the post-outburst wind? Also using spectropolarimetry we have shown that the winds of R127, AG Car & HR Car are axisymmetric today which indicates the post-eruption wind is probably asymmetric as well

Frank: That is a good point. I chose a spherical post-outburst wind for simplicity. Making it aspherical would however not change the qualitative effects seen in these models.

References

- Bjorkman, J & Cassinelli, J. 1992, ApJ, 409, 429
- Davidson, K, Ebbets, D, Weigelt, G, Humphreys, R, Hajian, A, Walborn, N, Rosa, M, 1995, AJ, 109, 1784
- Ebbets, D., Garner, H., White, R., Davidson, K, & Walborn, N 1993, in Circumstellar Meia in the Late Stages of Stellar Evolution, Proc. 34th Herstmonceux Conf. (Cambridge, Cambridge Univ. Press)
- Frank, A., Mellema, G. 1994, ApJ, 430 800
- Frank, A., Balick, B., Davidson, 1994, ApJ, 441L, 77 (FBD)
- Frank, A., Balick, B. & Livio 1996, ApJ, 471, L53
- Frank, A., & Mellema, G., 1996, ApJ, 472, 648
- Frank, A., Ryu, D. & Davidson 1997, ApJ, submitted
- Hester, J. J., Light, R. M., Westphal, J. A., Currie, D. G., Groth, E. J., 1991, AJ, 102, 654
- Humphreys, R., & Davidson, K., 1994, PASP, 106, 1025
- Lamers, H., & Pauldrach, A., 1991, A&A, 244L, 5
- Langer, N, Hamann, W-R., Lennon, M., Najarro, F., Pauldrach, A., Puls, J., 1994, A&A, 290, 819
- Leitherer, C, Allen, R, Altner, B, Daminieli, A., Drissen, L., Idiart, T, Lupie, O., Nota, A, Schmutz, W., Shore, S, 1994, ApJ, 428, 292
- Manchado, A, Guerrero, M., Stanghelli, L., & Serra-Ricart, M., 1996 "The IAC Catalog of Northern Galactic PNe", (IAC, La Laguna)
- Mac Low, M., Langer, N., & Garcia-segura, G., 1996,BAAS, 188, 3806 (MLG)
- Masson, C. R. & Chernin, L. M. 1992, ApJ, **387** L47
- Morse, J., Davidson, K, Ebbets, Walborn, N, 1996, preprint
- Nota, A., Livio, M, Clampin, M, Schulte-ladbeck, R., 1995, ApJ, 448, 788 (NLCS)
- Nota, A., Clampin, M, Pasquali, A., Pollacco, D., Scuderi, S, Livio, M, 1996, ApJ, 473, 946
- Owocki, S. Cranmer, S., Gayley, K. G. 1996 ApJ, 472L, 115
- Weis, K., Duschl, W., Bomans, D., Chu, Y-H., & Joner, M., 1996, A&A, in press

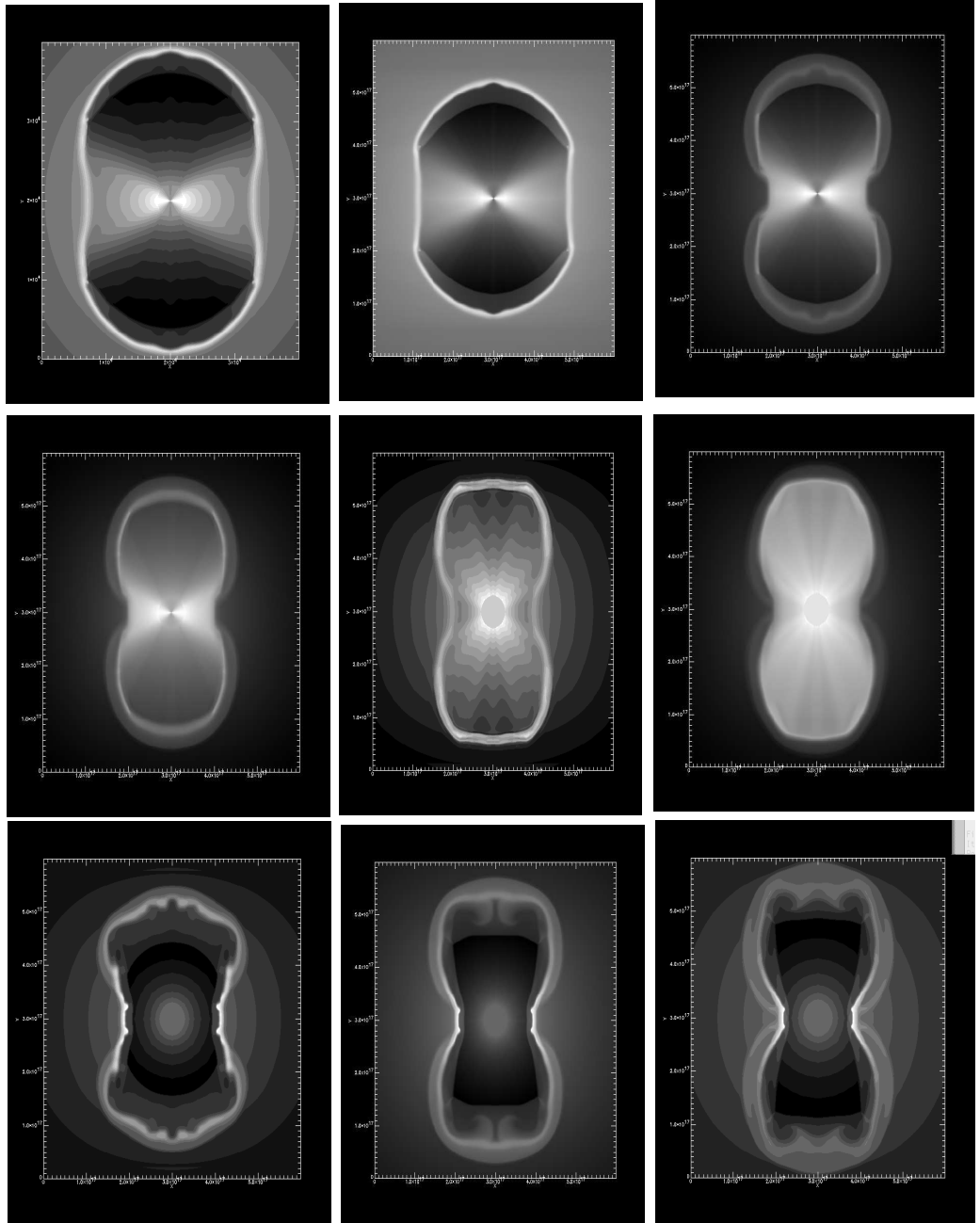


Fig 1. Log density maps for nine simulations. Each image shown represents a grid of size $R = Z = 1.2 \times 10^{18}$ cm on each side. The time at which each image was taken are (Upper = U; Middle = M; Lower = L; Right = r, middle = m; left = l): Run A (Ul) 802 y; Run B (Um) 802 y; Run C (Ur) 321 y; Run D (Mr) 240 y; Run E (Mm) 321 y; Run F (Ml) 200 y; Run H (Ll) 240 y; Run I (Lm) 250 y; Run J (Lr) 240 y